Novel Surface Modes in Spinodal Decomposition

Hans Peter Fischer, Philipp Maass, and Wolfgang Dieterich
Fakultät für Physik, Universität Konstanz, D-78457 Konstanz, Germany
(Received 23 December 1996)

We study the spontaneous phase separation of a binary mixture in the presence of a flat wall, focusing on the early stage of the demixing kinetics. Based on a Ginzburg-Landau type approach, we show the existence of novel unstable concentration waves with wave vectors $\vec{k}_{\parallel}$ parallel to the wall, which are characterized by a surface dispersion relation $\omega_s(k_{\parallel})$ and amplitudes $\overline{s}$ decaying exponentially into the bulk. The surface modes are superimposed on the laterally averaged concentration profile and are directly observable by experiment, if the wall right after a quench does not favor any of the two components of the mixture. [S0031-9007(97)03722-8]

PACS numbers: 64.75.+g, 05.70.Ln, 68.10.–m

The question of how the process of spontaneous phase separation in binary mixtures (spinodal decomposition; see, e.g., [1,2]) is influenced by the presence of walls has gained much attention recently both in experimental [3–8] and theoretical work [9–15]. The problem has mostly been studied for polymer mixtures although it might also be important in other systems, as, for example, in binary metallic alloys [16,17]. From a technological viewpoint, binary polymer mixtures are particularly interesting, since the occurring structures during the phase separation process may get frozen by a rapid quench into the glassy state. In this way microstructures at surfaces on very small length scales can be produced [18].

The experiments and theoretical studies quoted above have shown that if one of the two components (say, A) of a binary mixture AB is preferentially attracted by the wall, surface-directed spinodal decomposition waves (SDW) emerge with wave vectors normal to the wall. These waves represent laterally averaged concentration profiles and have their origin in the rapid formation of a layer of the A-rich phase next to the wall at the very beginning of the phase separation process.

In this Letter we focus on the opposite situation, where none of the two components A or B has initially a strong preference to be attracted (or repelled) by the wall. Experimentally, this situation may be realized, for example, by an appropriate choice of the surface material or by tuning the mixing ratio of the two components properly (see below). We will show that under such conditions of "neutral" walls, lateral surface structures can evolve, which have their origin in lateral surface modes (LSM) with wave vectors parallel to the wall. The LSM are characterized by a specific dispersion relation $\omega_s(k_{\parallel})$ and amplitudes decaying exponentially into the bulk. Both their dispersion relation and their decay lengths depend strongly on the surface properties. In fact, depending on the type of surface material, the formation of both SDW and lateral domain structures has been observed during spinodal decomposition of a blend of deuterated polystyrene and poly(styrene-co-4-bromostyrene) (PBr_xS) [5].

It is important to note that the LSM are always present even if one of the two components of the binary mixture is preferentially attracted by the wall. Within the linearized theory, the LSM represent the solution of a homogeneous boundary value problem, while the SDW can be regarded as originating from a particular integral of the corresponding inhomogeneous boundary value problem for vanishing wave vector parallel to the wall. The linear superposition of both solutions gives the general solution in real space. However, if the wall strongly favors one of the components, the LSM have amplitudes much smaller than the amplitude of the SDW, and therefore it might be difficult to resolve them by experiment.

Our starting point to describe spinodal decomposition in the presence of a wall is the time-dependent Ginzburg-Landau theory as used in previous theoretical work [9–15]. The wall is assumed to be a flat surface at $z = 0$. In the half space $z \geq 0$ the system is described by the local time-dependent order parameter $\psi(\vec{x}, t) = \psi(\vec{\rho}, z, t)$, representing, e.g., the normalized difference in local coarse grained concentrations of the two pure components of a binary polymer mixture. The free energy functional $F[\psi] = F_b[\psi] + F_s[\psi]$ is decomposed into a bulk contribution $F_b[\psi] = \int_{z>0} d^d x\, [\frac{1}{2}\sigma_b(\vec{\nabla}\psi)^2 + f_b(\psi)]$ and a surface contribution $F_s[\psi] = \int d^{d-1}\rho [\frac{1}{2}\sigma_s(\vec{\nabla}_\rho\psi)^2 + f_s(\psi)]_{z=0}$, where $f_b(\psi)$ and $f_s(\psi)$ are, respectively, the bulk and surface free energy densities, and the gradient terms take into account the influence of spatial order parameter fluctuations. The time-dependent Ginzburg-Landau equation (Cahn-Hilliard equation [19]) reads

$$\partial_t \psi = \Gamma_b \Delta[-\sigma_b \Delta\psi + f_b'(\psi)], \tag{1a}$$

where Γ_b is a (constant) bulk mobility and $f_b' = df_b/d\psi$. No thermal noise current has been added on the right-hand side; i.e., we assume that the system can be treated within the low noise limit (see, e.g., [20]). Equation (1a) has to be supplemented by two boundary conditions at $z = 0$ (for $z \to \infty$ one has to recover the bulk behavior). The first one is simply the condition that no current can flow through the

surface,

$$\partial_z[-\sigma_b\Delta\psi + f_b'(\psi)]_{z=0} = 0. \quad (1b)$$

The second boundary condition may be derived by requiring that the system tends to minimize its surface free energy,

$$\partial_t\psi|_{z=0} = -\Gamma_s[-\sigma_s\Delta_\rho\psi - \sigma_b\partial_z\psi + f_s'(\psi)]_{z=0}. \quad (1c)$$

Γ_s defines a surface kinetic coefficient and the term $\sigma_b\partial_z\psi$ is due to the surface contribution coming from the variation $\delta F_b[\psi]$ of the bulk free energy [21]. Boundary conditions of similiar form as Eqs. (1b) and (1c) have also been derived from a semi-infinite Ising model with Kawasaki spin exchange dynamics [11,22].

We now consider the system to be rapidly quenched at time $t = 0$ from a high temperature well above the coexistence curve to a low temperature inside the unstable region of the miscibility gap where $f_b''(\psi) < 0$. By ψ_0 we denote the homogeneous state before the quench and define $\hat{\phi}_{\vec{k}_\parallel}(z,t)$ as the Fourier transform of the fluctuation $\phi(\vec{\rho},z,t) = \psi(\vec{\rho},z,t) - \psi_0$ with respect to the lateral coordinates $\vec{\rho}$ [23]. Periodic boundary conditions in the lateral directions are imposed so that we can deal with discrete wave vectors $\vec{k}_\parallel$. By choosing the bulk correlation length $\xi_b = [\sigma_b/f_b''(\psi_1)]^{1/2}$ as the length unit and $\tau = \xi_b^2/\Gamma_b f_b''(\psi_1)$ as the time unit, where ψ_1 is the equilibrium value corresponding to the A-rich phase, Eqs. (1a)–(1c) become after linearization

$$[\partial_t + (\partial_z^2 - k_\parallel^2)(\partial_z^2 + k_c^2 - k_\parallel^2)]\hat{\phi}_{\vec{k}_\parallel} = 0, \quad (2a)$$

$$\partial_z[\partial_z^2 + k_c^2 - k_\parallel^2]_{z=0}\hat{\phi}_{\vec{k}_\parallel} = 0, \quad (2b)$$

$$[\tilde{\Gamma}_s^{-1}\partial_t - \partial_z + \tilde{\sigma}_s k_\parallel^2 + g]_{z=0}\hat{\phi}_{\vec{k}_\parallel} = h\delta_{\vec{k}_\parallel,\vec{0}}. \quad (2c)$$

We have introduced $g = f_s''(\psi_0)/f_b''(\psi_1)\xi_b$, $h = -f_s'(\psi_0)/f_b''(\psi_1)\xi_b$, $\tilde{\sigma}_s = \sigma_s/f_b''(\psi_1)\xi_b^3$, $\tilde{\Gamma}_s = \xi_b^3\Gamma_s/\Gamma_b$, and the critical wave number $k_c = [-f_b''(\psi_0)/f_b''(\psi_1)]^{1/2}$ of the bulk modes (for $k < k_c$ the bulk modes are unstable). Equations (2a)–(2c) represent an inhomogeneous boundary value problem with the inhomogeneity only appearing for $k_\parallel = 0$, and the SDW (in the linear regime) can be regarded as the particular integral satisfying the initial condition $\hat{\phi}_{\vec{k}_\parallel=0}(z,0) = 0$.

The homogeneous problem is solved by a separation ansatz, yielding modes of the form $\hat{\phi}_{\vec{k}_\parallel}(z,t) = e^{\omega t}\sum_j a_j e^{-\kappa_j z}$. For given ω, Eq. (2a) determines four possible values of κ_j by the condition $\kappa_j^2 = k_\parallel^2 - k_m^2 \pm i(\omega - \omega_m)^{1/2}$, where $k_m = k_c/\sqrt{2}$ and $\omega_m = k_m^4$ are the wave number and growth rate of the most unstable bulk mode, respectively. To obtain a physical solution $\hat{\phi}_{\vec{k}_\parallel}(z,t)$, we have to require $a_j = 0$ if Re $\kappa_j < 0$. The boundary conditions (2b) and (2c) then constitute a homogeneous system of linear equations for the remaining amplitudes a_j. The condition for this system to have a nontrivial solution yields the spectrum of allowed modes. Different types of modes can occur: Surface modes with Re $\kappa_j > 0$ for all j yielding the LSM, as well as pure bulk modes with Re $\kappa_j = 0$ for all j. The remaining modes are bulk modes, which are modified near the surface. While for $\omega > \omega_m$ only surface modes are possible, the spectrum for $\omega \le \omega_m$ consists of both bulk and surface modes, which will be discussed elsewhere [24].

Here we concentrate on the regime $\omega > \omega_m$, where the surface modes are more unstable than any bulk mode. One can show that a necessary condition for such a solution to exist is $\omega/\tilde{\Gamma}_s < -g - \tilde{\sigma}_s k_\parallel^2$, which requires $g < 0$. For this type of LSM we then obtain two complex conjugate values $\kappa_{1,2} = \gamma \pm iq$, with $2^{1/2}\gamma = \{(k_\parallel^2 - k_m^2) + [(k_\parallel^2 - k_m^2)^2 + (\omega - \omega_m)]^{1/2}\}^{1/2} > 0$ and $2^{1/2}q = \{-(k_\parallel^2 - k_m^2) + [(k_\parallel^2 - k_m^2)^2 + (\omega - \omega_m)]^{1/2}\}^{1/2}$. The LSM can now be written as $\hat{\phi}_{\vec{k}_\parallel}(z,t) = [\alpha_1\cos(qz) + \alpha_2 \times \sin(qz)]e^{-\gamma z + \omega t}$, where α_1 and α_2 are determined by

$$\begin{bmatrix} \omega\tilde{\Gamma}_s + \tilde{\sigma}_s k_\parallel^2 + g + \gamma & -q \\ \chi_-(\gamma,q) & \chi_+(q,\gamma) \end{bmatrix}\begin{pmatrix} \alpha_1 \\ \alpha_2 \end{pmatrix} = 0 \quad (3)$$

and $\chi_\pm(\gamma,q) = \gamma^3 - 3\gamma q^2 \pm (k_\parallel^2 - k_c^2)\gamma$. Note that the solubility condition of Eq. (3) leads to an implicit equation for the dispersion relation $\omega_s(k_\parallel)$, as γ and q depend on ω and $k_\parallel$. After inserting $\omega = \omega_s(k_\parallel)$ in the expressions for γ, q, and $\eta \equiv \alpha_2/\alpha_1$ derived above, these quantities become functions of $k_\parallel$ only. The explicit form of the LSM is then $\hat{\phi}_{\vec{k}_\parallel} = c_{\vec{k}_\parallel}\exp[\omega_s(k_\parallel)t - \gamma(k_\parallel)z]\{\cos[q(k_\parallel)z] + \eta(k_\parallel)\sin[q(k_\parallel)z]\}$, where $c_{\vec{k}_\parallel}$ is determined by the initial condition.

As an example we choose for the (rescaled) bulk and surface free energy densities $\tilde{f}_b(\psi) = f_b(\psi)/f_b''(\psi_1) = -\frac{1}{4}\psi^2 + \frac{1}{8}\psi^4$ and $\tilde{f}_s(\psi) = f_s(\psi)/\xi_b f_b''(\psi_1) = -h_s\psi + \frac{1}{2}g_s\psi^2$ at the final temperature after the quench, which gives $h = h_s - g_s\psi_0$ and $g = g_s$. The resulting dispersion relation $\omega_s(k_\parallel)$ is shown in Fig. 1 for fixed $\tilde{\Gamma}_s = 10$, $g_s = -4$, and various values of $\tilde{\sigma}_s$. For $\tilde{\sigma}_s \lesssim 0.25$, $\omega_s(k_\parallel)$ displays a maximum at $k_{\parallel m}$ larger than $k_m = 1/2$ with $\omega_s(k_{\parallel m}) > \omega_m = 1/16$, while for $\tilde{\sigma}_s \gtrsim 0.5$, $\omega_s(k_\parallel)$ has its maximum at $k_\parallel = 0$. Accordingly, we expect the appearance of surface domains with a lateral length scale, which for $\tilde{\sigma}_s \lesssim 0.25$ is smaller than the bulk domain size but larger for $\tilde{\sigma}_s \gtrsim 0.5$.

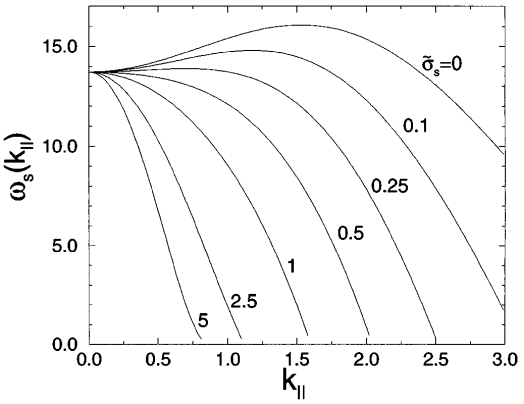

FIG. 1. Surface dispersion relation $\omega_s(k_\parallel)$ of the LSM for $\tilde{\Gamma}_s = 10$, $g_s = -4$, and various values of $\tilde{\sigma}_s$.

Next we test these predictions of the linearized theory against numerical calculations for the discretized nonlinear Eqs. (1a)–(1c). For convenience these calculations are carried out for a two-dimensional symmetric slab of size $L_x \times L_z = 40\xi_b \times 80\xi_b$ (using a grid with 3.2×10^5 points). The width L_z is chosen sufficiently large such that the surface structures emerging from the two walls do not interfere. Periodic boundary conditions are used in the x direction. The system is quenched at $\psi_0 = 0$ (critical quench) and the initial configuration $\psi(x, z, 0)$ right after the quench consists of uniformly distributed random fluctuations of amplitude $A = \pm 0.01$ [25].

Figure 2 shows domain structures obtained from the numerical calculations for $h_s = 0$ and the same parameters $\tilde{\Gamma}_s = 10$, $g_s = -4$ as in Fig. 1. The patterns in Figs. 2(a) and 2(b) correspond to $\tilde{\sigma}_s = 0$ and to two progressive times $t = 0.25$ and $t = 0.5$, while the analogous results for $\tilde{\sigma}_s = 5$ are shown in Figs. 2(c) and 2(d). In all cases isotropic structures in the bulk with domains of size $2\pi/k_m \simeq 12$ separate anisotropic domain structures occurring near the walls, which are induced by the LSM. The typical lateral length scales are as expected from the dispersion relation discussed above: In Figs. 2(a) and 2(b) the length scales are shorter than in the bulk, while in Figs. 2(c) and 2(d) a different morphology of surface domains is seen with lateral length scales larger than in the bulk. Also the typical extension of surface domains in the z direction differs from that of the bulk domains and is approximately given by $2\pi/q(k_{\|m})$. (From the theory we get $2\pi/q(k_{\|m}) \simeq 5.7$ and 4.5 for $\tilde{\sigma}_s = 0$ and 5, respectively, in good agreement with the patterns shown.) The LSM dominate the domain structure up to a distance l_{LSM} from the walls, where the amplitude of the most unstable LSM ($\sim e^{\omega_s(k_{\|m})t - \gamma(k_{\|m})z}$) becomes comparable to that of the most unstable bulk mode ($\sim e^{\omega_m t}$), yielding $l_{\mathrm{LSM}} \simeq [\omega_s(k_{\|m}) - \omega_m]t/\gamma(k_{\|m})$. Accordingly, with increasing time the surface structures extend farther into the bulk, as can be seen by comparing Figs. 2(a) and 2(c) ($l_{\mathrm{LSM}} \simeq 3.4$) with Figs. 2(b) and 2(d) ($l_{\mathrm{LSM}} \simeq 6.9$), respectively.

For a more quantitative analysis, we show in Fig. 3 the normalized first moment $I(z,t) = \int dk_{\|} k_{\|} S_{k_{\|}}(z,t) / \int dk_{\|} S_{k_{\|}}(z,t)$ of the lateral structure factor $S_{k_{\|}}(z,t) = \langle \hat{\phi}_{\vec{k}_{\|}}(z,t) \hat{\phi}^{\star}_{\vec{k}_{\|}}(z,t) \rangle$ as a function of z at the same time $t = 0.5$ and the same surface parameters as in Figs. 2(b) and 2(d) [$\langle \cdots \rangle$ denotes an average over many different initial configurations $\psi(x, z, 0)$]. The inverse $I^{-1}(z,t)$ is a measure of the characteristic lateral domain size at position z and time t. The solid lines in the figure refer to the numerical results, while the dashed lines are calculated from the linear theory presented above. Only the modes with $\omega > \omega_m$ have been included in the calculation, which dominate the behavior for small z. As can be seen from Fig. 3, $I(z,t)$ exhibits oscillations for small $z \lesssim l_{\mathrm{LSM}}$, which are caused by the oscillatory behavior of the LSM as a function of z and are reproduced by the linear theory to a good approximation [26]. For $z \gtrsim l_{\mathrm{LSM}}$, $I(z,t)$ approaches the value $k_m = 1/2$, as expected in the bulk. (This behavior is not reproduced by the dashed line, since we did not include the bulk modes in our calculation.)

It is clear that a good agreement between the calculated and simulated moments $I(z,t)$ can no longer be expected at later times due to the nonlinear terms in Eqs. (1a)–(1c). In general, nonlinearities, thermal noise, and finite quench rates limit the validity of the linearized theory [2]. Assuming an instantaneous quench, we can estimate a critical time t_{cr}, where the linear theory ceases to be valid, by comparing the size of the nonlinear terms in Eqs. (1a)–(1c) with the linear ones. In our case, where the order parameter at the surface grows faster than in the bulk, this yields $t_{\mathrm{cr}} \approx |\ln A/\omega_s(k_{\|m})|$, where A denotes the amplitude of the initial order parameter fluctuations (see above). For the parameters chosen in Fig. 2 we thus obtain $t_{\mathrm{cr}} \approx \tau$. We note that τ can become quite large in mixtures of polymers with high molecular weight, where the linear theory may remain applicable up to times of order hours [27].

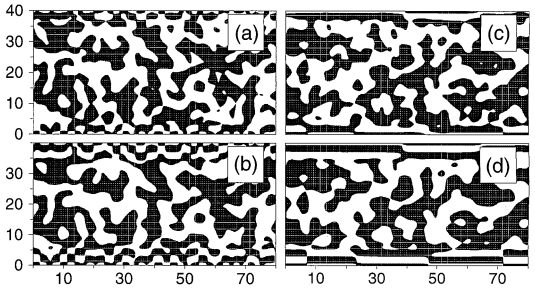

FIG. 2. Domain structures after a critical quench for (a) $\tilde{\sigma}_s = 0$, $t = 0.25$, (b) $\tilde{\sigma}_s = 0$, $t = 0.5$, (c) $\tilde{\sigma}_s = 5$, $t = 0.25$, and (d) $\tilde{\sigma}_s = 5$, $t = 0.5$. Surface parameters $\tilde{\Gamma}_s = 10$, $g_s = -4$ are chosen as in Fig. 1, and $h_s = 0$. Black areas refer to $\psi(x,z,t) > 0$ and white areas to $\psi(x,z,t) < 0$.

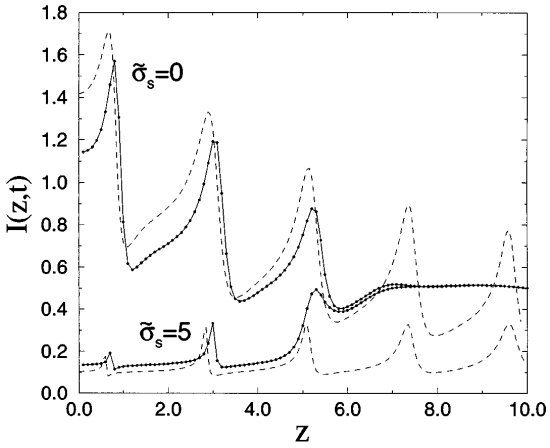

FIG. 3. Normalized first moment $I(z,t)$ of the lateral structure factor as a function of z at fixed $t = 0.5$ for the same surface parameters as in Fig. 2. The symbols mark the result from simulations of Eqs. (1a)–(1c), and the solid line is drawn as a guide for the eye. Averages were performed over 10 different initial configurations $\psi(x, z, 0)$ and both walls of the slab. The dashed lines indicate the results from the linear theory, where only the LSM with $\omega_s > \omega_m$ are taken into account.

Finally, we have to make some remarks on our choice of the surface parameters. The choice $h_s = 0$ with $\psi_0 = 0$ implies $h = 0$, and accordingly no SDW occurs. For large h, in contrast, the SDW would dominate the domain pattern, but the LSM may still be observable in the fluctuations *after substracting* the laterally averaged concentration profile. This method, however, should work well only in the early stage of the phase separation. In later stages, the modes interact with each other and with the SDW through the nonlinearities, which leads to coarsening of both surface and bulk domains. It would be interesting to see how the coupling to the SDW influences the scaling behavior of $S_{k_\parallel}(z, t)$ in the late stage. Clearly, the most direct way to observe the LSM experimentally is to suppress the SDW by choosing neutral walls, i.e., $h \simeq 0$. One possibility to vary $h \propto f_s'(\psi_0)$ is by changing ψ_0. Moreover, it has been shown that surface interactions can be modified to a large extent by grafting techniques [28].

The values $\tilde{\Gamma}_s = 10$ and $g_s = g = -4$ have been chosen such that a range of $k_\parallel$ values exists, where $\tilde{\Gamma}_s(-g - \tilde{\sigma}_s k_\parallel^2) \gg \omega_m$ is satisfied, allowing us to exemplify the case where surface modes occur that are more unstable than the bulk modes. It is important to note that the identity $g_s = g$ is a consequence of the special form of $\tilde{f}_s(\psi)$ chosen. In general, $g \propto f_s''(\psi_0)$ characterizes the effective strength of the interaction between the mixture components near the wall right after the quench. A negative sign of g corresponds to enhanced couplings, which, for example, can occur in fcc binary alloys with competing interactions in the bulk [17]. In the case $g > 0$, the LSM would not be more unstable than the bulk modes. However, by extending our analysis to a slab geometry [24], one finds the LSM to become important even for $g > 0$. The LSM give rise to new characteristic length scales in the directions parallel and perpendicular to the walls, which in sufficiently narrow slabs can determine the overall domain structure. In fact, recent experiments in ultrathin films show a transition from a homogenous in-plane distribution of the order parameter to pronounced lateral structures as the film thickness is reduced [29].

We thank H. L. Frisch, A. Majhofer, U. Steiner, and S. Walheim for very helpful discussions and the Deutsche Forschungsgemeinschaft (SFB 513) for financial support.

[1] J. D. Gunton, M. San Miguel, and P. S. Sahni, in *Phase Transitions and Critical Phenomena*, edited by C. Domb and J. L. Lebowitz (Academic Press, London, 1983), Vol. 8, p. 267.
[2] K. Binder, in *Materials Science and Technology*, edited by R. W. Cahn, P. Haasen, and E. J. Kramer (VCH, Weinheim, 1991), Vol. 5, p. 405.
[3] R. A. L. Jones, L. J. Norton, E. J. Kramer, F. S. Bates, and P. Wiltzius, Phys. Rev. Lett. **66**, 1326 (1991).
[4] P. Wiltzius and A. Cumming, Phys. Rev. Lett. **66**, 3000 (1991).
[5] F. Bruder and R. Brenn, Phys. Rev. Lett. **69**, 624 (1992).
[6] H. Tanaka, Phys. Rev. Lett. **70**, 53 (1993).
[7] B. Q. Shi, C. Harrison, and A. Cumming, Phys. Rev. Lett. **70**, 206 (1993).
[8] G. Krausch, C. A. Dai, E. J. Kramer, and F. Bates, Phys. Rev. Lett. **71**, 3669 (1993).
[9] G. M. Xiong and C. D. Gong, Phys. Rev. B **39**, 9384 (1989).
[10] R. C. Ball and R. L. H. Essery, J. Phys. Condens. Matter **2**, 10 303 (1990).
[11] S. Puri and K. Binder, Phys. Rev. A **46**, R4487 (1992); Phys. Rev. E **49**, 5359 (1994).
[12] G. Brown and A. Chakrabarti, Phys. Rev. A **46**, 4829 (1992).
[13] J. F. Marko, Phys. Rev. E **48**, 2861 (1993).
[14] C. Sagui, A. M. Somoza, C. Roland, and R. C. Desai, J. Phys. A **26**, L1163 (1993).
[15] A. Bhattacharya, M. Rao, and A. Chakrabarti, Phys. Rev. E **49**, 524 (1994).
[16] K. R. Mecke and S. Dietrich, Phys. Rev. B **52**, 2107 (1995).
[17] W. Schweika, K. Binder, and D. P. Landau, Phys. Rev. Lett. **65**, 3321 (1990).
[18] G. Krausch, Mater. Sci. Eng. **R14**, 1 (1995).
[19] J. W. Cahn and J. E. Hilliard, J. Chem. Phys. **28**, 258 (1958); **31**, 688 (1959).
[20] T. M. Rogers, K. R. Elder, and R. C. Desai, Phys. Rev. B **37**, 9638 (1988).
[21] Within a more microscopic approach one can show that a term $\propto \vec{\nabla}_\rho \cdot \vec{j}_s$ should be added on the left-hand side of Eq. (1c), which depends on the order parameter ψ and its derivatives. However, this term, which describes the conserved diffusional dynamics within the surface layer next to the wall, leads only to a renormalization of the surface parameter $\vec{\sigma}_s$ in the corresponding linearized Eq. (2c), if derivatives of higher than second order are neglected.
[22] K. Binder and H. L. Frisch, Z. Phys. B **84**, 403 (1991).
[23] For simplicity we have not taken into account that ψ_0 will in general depend on z near the surface at the temperature before the quench.
[24] H. P. Fischer, W. Dieterich, and P. Maass (to be published).
[25] In the numerical scheme, the space derivatives in Eqs. (1a)–(1c) were approximated up to second order in the grid spacing Δ_x. In order to resolve the smallest length scales at the surface (which, for the parameters chosen, are approximately set by the penetration depth of the most unstable LSM), we had to choose $\Delta_x = \xi_b/10$. For the integration in time, Euler's method with a very small time step $\Delta_t = 2.5 \times 10^{-6}\tau$ was used to avoid numerical instabilities.
[26] The deviations are not only caused by the nonlinearities. Calculations with varying grid size Δ_x show that the agreement between theory and numerics can be slightly improved by using smaller Δ_x. However, in achieving full convergence we were limited by the available computing time ($\sim \Delta_x^{-6}$).
[27] T. Hashimoto, Phase Trans. **12**, 47 (1988).
[28] E. Delamarche, B. Michel, H. A. Biebuyck, and C. Gerber, Adv. Mater. **8**, 9 (1996).
[29] L. Sung, A. Karim, J. F. Douglas, and C. C. Han, Phys. Rev. Lett. **76**, 4368 (1996).